Investigations of some elastic and shielding properties of barium zinc phosphate glass containing lead ions

E. Banoqitah[a,b], F. Djouider[a,b], M. R. Alnowaimi[a,b], A. M. Alhawsawi[a,b], E. B. Moustafa[c], A. H. Hammad[d,*]
[a]*Nuclear Engineering Department, Faculty of Engineering, King Abdulaziz University, P.O. Box 80204, Jeddah 21589, Saudi Arabia*
[b]*Center for Training & Radiation Prevention, King Abdulaziz University, P.O. Box 80204, Jeddah, 21589, Saudi Arabia*
[c]*Mechanical Engineering Department, Faculty of Engineering, King Abdulaziz University, P.O. Box 80204, Jeddah 21589, Saudi Arabia*
[d]*Center of Nanotechnology, King Abdulaziz University, Jeddah 21589, Saudi Arabia*

The current research focuses on improving some of the physical and radiation properties of barium zinc phosphate glass containing lead oxide. The Makishima-Mackenzie model evaluates the elastic parameters. The XCOM database simulation predicts the shielding properties. Furthermore, the glass composition and the simulated X-ray or gamma-ray energy predict the shielding behavior. The optimal thickness for all glass samples to achieve a 90% reduction in intensity at an energy of 59.54 keV is 5.2 mm. These glasses have great potential as materials for shielding against gamma and X-rays.

(Received April 30, 2024; Accepted July 12, 2024)

Keywords: Phosphate glass, Lead ions, Elastic properties, Shielding properties.

1. Introduction

Phosphate glasses are promising vitreous materials for a wide range of different technological applications, such as laser host [1], glass-metal sealing [2], ionic conducting materials [3], biocompatible materials [4], and radiation technology [5]. On the other hand, the hygroscopic nature and weak chemical durability of phosphate glasses restrict their applications. However, the introduction of certain metal oxides to phosphate networks improves and enhances the chemical durability of such materials [6].

For the purpose of manufacturing radiation shield materials, glasses made of heavy metal oxides have been constructed. In addition to their transparency and hardness, they are also capable of effectively absorbing radiation, which allows them to overcome the limitations of traditional and opaque materials [7, 8]. The rigidity of glass demonstrates the structural toughness and stability of the material. In general, the rigidity of glass can be approximated through the examination of its mechanical and elastic properties [9].

The purpose of this study is to investigate the elasticity and shielding properties of barium zinc phosphate glass that contains varying concentrations of lead oxide. In this study, the behavior of the glass density is used to figure out important elastic parameters and the mass attenuation coefficient by running a Monte Carlo simulation.

2. Experimental details

The melt-annealing technique was used to prepare barium zinc aluminum phosphate glass. The high chemical quality, greater than 99% purity, of zinc oxide (ZnO), aluminum oxide (Al_2O_3),

* Corresponding author: ahhhassan@kau.edu.sa
https://doi.org/10.15251/JOR.2024.204.483

barium carbonate ($BaCO_3$) as a source of barium oxide (BaO), lead oxide (Pb_3O_4) as a source of lead oxide (PbO), and ammonium dihydrogen phosphate ($NH_4H_2PO_4$) as a source of phosphate (P_2O_5). PbO was introduced at the expense of BaO with an increment of 5 mol%. ZnO, Al_2O_3, and P_2O_5 ratios are fixed and become 25, 5, and 55 mol%, respectively. The samples labeled are free PbO (0 PbO), 5 PbO, 10 PbO, and free BaO (15 PbO). After weighing the appropriate chemicals, they were mixed, placed in a 100-ml porcelain crucible, and melted in an electrical furnace at 1250 °C for 120 minutes. The mixture was stirred several times to obtain homogenity. Finally, the melt was poured into a preheated mold at 400 °C for 180 minutes and allowed to cool to room temperature.

The experimental glass density (D_{exp}) for various samples was measured using the Archimedes method. The weight of the sample was recorded both in air and when submerged in a stable liquid (xylene). Each sample performed three measurements to determine the level of uncertainty.

3. The elastic parameters

The elastic properties of a material can be deduced from its physical properties. Makishima and Mackenzie [10, 11] proposed the essential features of calculating the elastic parameters based on two important physical parameters: the dissociation energy per unit volume (G_i) and the ionic packing ratio (V_P). The ionic packing ratio is dependent on the glass density (D_{exp}) according to the following equation [12, 13]:

$$V_P = D_{exp} \times \frac{\sum V_i x_i}{\sum M_i x_i} \tag{1}$$

where V_i, M_i, and x_i are the packing density, the molecular weight, and the molar ratio of an oxide (M_uO_y), and the following formula is used to calculate V_i:

$$V_i = \frac{4}{3}\pi N_A \times (uR_M^3 + yR_O^3) \tag{2}$$

in which R_M and R_O are the Shannon's ionic radii of the cation (M) and the anion (O) [14, 15]. The R_O is equal to 1.4 Å, and the ionic radii of Zn, Al, P, Ba, and Pb are 0.6, 0.53, 0.17, 1.36, and 1.18 Å, respectively.

The elastic parameters used in the current investigation are Poisson's ratio (σ), Young's (E), bulk (B), and shear (S) moduli from the following equations [10, 11]:

$$\sigma = \frac{1}{2} - \frac{1}{7.2V_P} \tag{3}$$

$$E = 8.36V_P \sum G_i x_i \tag{4}$$

$$B = 10\, V_P^2 \sum G_i x_i \tag{5}$$

$$S = \frac{30\, V_P^2}{10.2V_P - 1} \sum G_i x_i \tag{6}$$

The Vickers hardness (H_v) of a glass is calculated using the following equation:

$$H_v = C(\eta BS)^{\frac{1}{2}} \tag{7}$$

where C is a constant equal to 0.15 calculated using the Yamane-Mackenzie procedure [16]. The relative bond strength factor (η) computed from the equation:

$$\eta = \frac{\sum(f_i q_i \epsilon_i)}{\epsilon_P \sum(f_i q_i)} \tag{8}$$

where f_i denotes the respective mole fraction of cations (M) in one mole of glass, q_i denotes the coordination numbers of glass cations, and ϵ_i denotes the single bond strengths (M–O) in kcal.

4. Shielding simulation

XCOM: Photon Cross Sections Database is the most widely used database for simulating and computing mass attenuation coefficients (μ_m) [17, 18]. By theoretically taking into account all of the material's interactions with photons, XCOM is a software tool that determines the total mass attenuation coefficients of any element, compound, or mixture from 1 keV to 10^2 GeV. It should be noted that the agreement between the experimental and simulated results has been verified with an error margin of ±3% [19]. The μ_m was calculated for X-rays with energies between 80.04 and 50.38 KeV and for gamma (γ-) rays with energies between 59.54 KeV and 2.506 MeV. The XCOM simulation needs the weight fraction of each component in composite materials to predict the overall attenuation coefficients.

The μ_m of the glass is then obtained from the XCOM database, and the following equations are used to calculate the other radiation shielding parameters [20-23]:

$$LAC\ (cm^{-1}) = \mu_m \times D_{exp} \tag{9}$$

$$t_{MFP}\ (cm) = 1/LAC \tag{10}$$

$$t_{HVL}\ (cm) = 0.693 \times t_{MFP} \tag{11}$$

$$t_{TVL}\ (cm) = 2.303 \times t_{MFP} \tag{12}$$

5. Results and discussion

Table 1 shows the response of the D_{exp} when PbO is added to the network. The D_{exp} values are influenced by the PbO ratio, which rises as the PbO content increases from 2.422 g/cm^3 to 3.636 g/cm^3. This trend involves substituting low-density BaO (5.72 g/cm^3) with high-density PbO (9.53 g/cm^3). These values are in line with the reported density values of zinc barium lead phosphate glasses [6, 24, 25].

The deformation brought on in axes that are orthogonal to the direction of loading is demonstrated via the Poisson's ratio (σ). The σ values are commonly less than 0.5 in glasses, which determines how the glass cross-linking network acts. A high degree of cross-linking exists in the glass if σ is between 0.1 and 0.2, and the σ values between 0.3 and 0.5 indicate low cross-linking of the glass [26, 27]. As shown in Table 1, the σ of the free PbO sample is 0.198 and increases as PbO is introduced and added to the phosphate network, reaching 0.28 at high PbO content (the free BaO sample). As a result, the zinc phosphate glass that has been prepared has a high cross-linked density. However, the addition of PbO could create some non-bridging oxygen linkages and change some Q^3 phosphate modes to Q^2 modes in the barium zinc phosphate glass system.

Fig. 1 shows the behavior of the other elastic parameters such as E, B, S, and H_v. The values of all elastic parameters for various glass compositions are listed in Table 1. The Young's modulus (E) is the modulus of elasticity, which measures the tensile or compressive stiffness when a lengthwise force is applied. The free BaO sample possesses a high elasticity of 69.648 GPa. As

shown in Fig. 1, the intercalation of PbO into the host glass increases the tensile or compressive stiffness. In addition, E is dependent on the properties of the glass, including the packing density ratio (V_P) and the dissociation energy per unit volume ($\sum G_i x_i$). Although the dissociation energy decreased from 13.695 to 13.17 when the glass composition changed from free PbO to free BaO, the E values increased as the V_P values increased from 0.46 to 0.62. The current E behaves differently from the ternary glass systems $40P_2O_5$–(60-x)ZnO–xPbO and $50P_2O_5$–(50-x)ZnO–xPbO [28]. According to Sidek et al. [28], the E values for both glass systems decreased as the PbO content increased, from 51.76 GPa to 38.53 GPa and from 46.06 GPa to 37.21 GPa, respectively.

The bulk (B) and shear (S) moduli describe how glass resists compression and deformation when a parallel external force is applied to one of its surfaces. The B and S values of the free PbO sample were 29.148 GPa and 23.597 GPa, which increased to 52.702 GPa and 29 GPa, respectively, when PbO was added. This means that PbO strengthens the elastic properties of zinc phosphate glasses, which can resist compression and deformation up to 52.7 GPa and 29 GPa, respectively, when external forces are applied. According to equation (7), glass hardness values are determined by the B and S moduli. When the BaO in the glass was completely replaced with PbO, the hardness increased from 3.37 GPa to 4.954 GPa. This behavior is related to Poisson's ratio, which is associated with an increase in the cross-linking density of glass.

Fig. 2 illustrates the behavior of the μ_m at different ranges of photon energies for X-rays and gamma rays. The behavior exhibited a decrease in μ_m as the energy increased in both X- and gamma rays. The μ_m decreased from 87.25 to 2.794 cm^2/g for the free PbO sample when the characteristic X-ray energies increased from 8.04 KeV to 50.37 KeV. The same trend in μ_m was observed for the gamma-ray energies from 59.54 KeV to 2.506 MeV, which decreased from 1.828 to 0.039 cm^2/g. In addition, the introduction of PbO at the expense of BaO led to a rise in the values of μ_m, as shown in Fig. 2. The μ_m values increased from 34.26 to 53.07 cm^2/g when the PbO content rose from 0 to 15% at X-ray energy of 13.37 KeV and from 0.07618 to 0.08368 cm^2/g at gamma-ray energy of 661.7 KeV. Moreover, in the gamma-ray characteristics, there is a sharp peak at 98.97 KeV, which is more clear at high PbO content. This could be related to the K-absorption edge of Pb. In general, in the energy range of 8.04 KeV–0.1 MeV, the photoelectric absorption process dominates the μ_m behavior, which attributes the sharply decreasing μ_m values to an increase in photon energy, where the partial cross section is associated with $1/E^{3.5}$ [39-33]. When the photon energy exceeds 0.1 MeV up to 2.506 MeV, the Compton scattering process dominates the μ_m behavior. The cross section is proportional to the inverse of the photon energy in this energy range [29-33]. Therefore, the μ_m of the free BaO samples had higher values than the free PbO samples.

Table 1. The ionic packing ratio (V_P), the dissociation energy per unit volume ($\sum G_i x_i$), relative bond strength factor (η), and the elastic parameters [Poisson's ratio (σ), Young's modulus (E), bulk modulus (B), shear modulus (S), and hardness value (H_v)].

	Free PbO	**PbO5**	**PbO10**	**Free BaO**
Glass Density (D_{exp}) (g/cm^3)	2.422	2.987	3.198	3.646
Ionic packing ratio (V_P)	0.461	0.551	0.572	0.633
Dissociation energy per unit volume ($\sum G_i x_i$) (Kcal/cm^3)	13.695	13.520	13.345	13.170
Relative bond strength factor (η)	0.734	0.726	0.721	0.714
Poisson's ratio (σ)	0.198	0.248	0.257	0.280
Young's modulus (E) (GPa)	52.820	62.295	63.816	69.648
Bulk modulus (B) (GPa)	29.148	41.070	43.664	52.701
Shear modulus (S) (GPa)	23.597	26.658	27.095	29.000
Hardness value (H_v) (GPa)	3.371	4.233	4.380	4.954

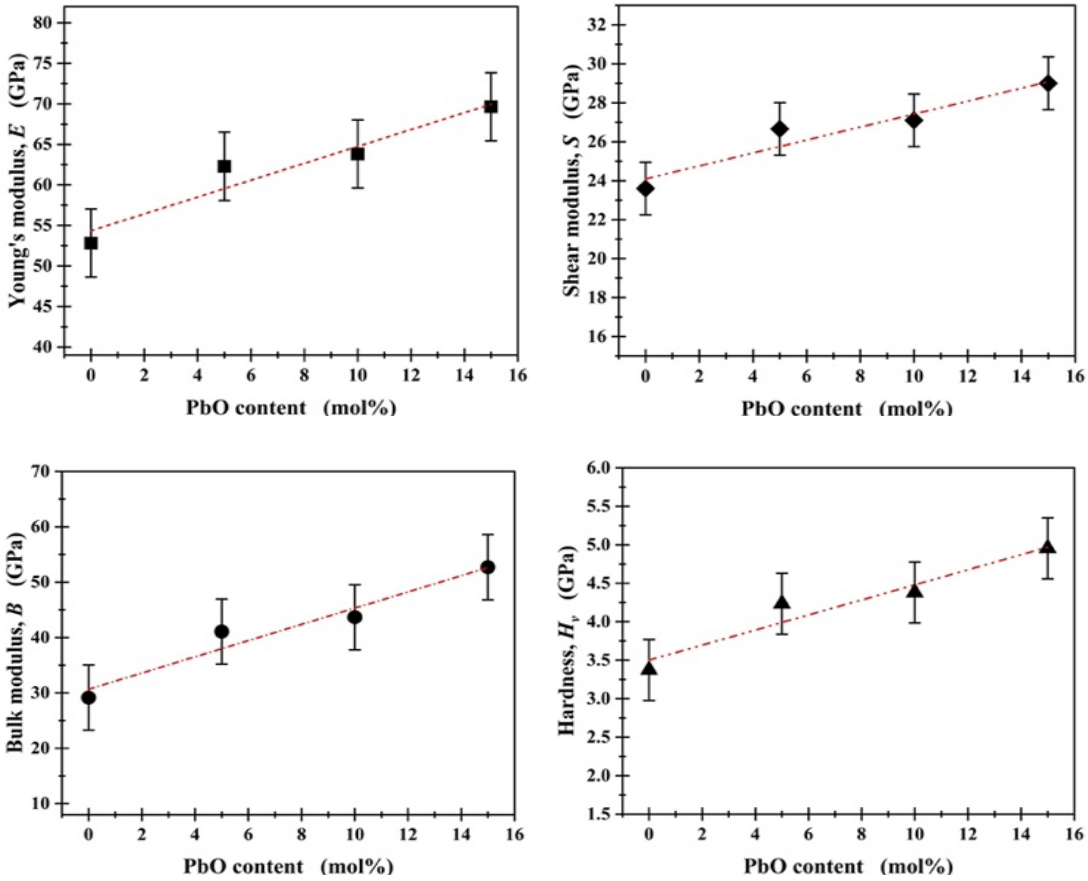

Fig. 1. The dependence of the elastic properties on the PbO concentration.

As shown in equation (9), the linear attenuation coefficient (*LAC*) reflects the μ_m behavior and the glass density (D_{exp}). Table 2 shows the values of *LAC* at different *X*- and gamma-ray energies for the samples. The PbO content affects the *LAC* values; it increases from the free PbO sample to the free BaO sample from 211.3195 cm^{-1} to 300.1387 cm^{-1} at 8.04 KeV and from 0.0946 cm^{-1} to 0.1465 cm^{-1} at 2.506 MeV, respectively. As shown in equations (10, 11, and 12), the values of *LAC* are crucial in order to calculate the other radiation parameters, such as t_{MFP}, t_{HVL}, and t_{TVL}.

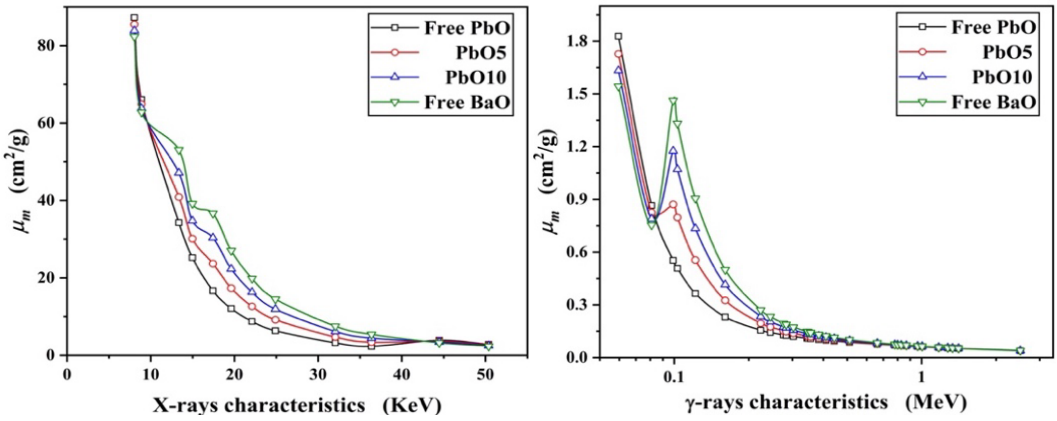

Fig. 2. Dependence of the μ_m on the photon energy for different glass compositions.

Table 2 The LAC values of $ZnO–P_2O_5$ glass containing BaO and PbO at different photon energies.

Photon energy, *E* (MeV)	***LAC* (cm^{-1})**			
	Free PbO	**PbO5**	**PbO10**	**Free BaO**
0.00804	211.3195	255.3885	268.2162	300.1387
0.01337	82.9777	122.0189	150.6897	193.4932
0.0221	21.1392	37.6959	52.1593	72.2272
0.03639	5.5294	10.0632	14.0712	19.6081
0.04448	9.2907	10.7920	10.8827	11.6817
0.05038	6.7670	7.8617	7.9310	8.5170
0.05954	4.4274	5.1585	5.2223	5.6257
0.081	2.0947	2.4666	2.5235	2.7501
0.09897	1.3379	2.6046	3.7608	5.3340
0.103	1.2298	2.3803	3.4250	4.8564
0.2234	0.3761	0.5839	0.7473	0.9840
0.3029	0.2906	0.4134	0.4985	0.6289
0.4111	0.2384	0.3196	0.3680	0.4473
0.511	0.2111	0.2753	0.3098	0.3697
0.6617	0.1845	0.2354	0.2600	0.3050
0.7789	0.1697	0.2146	0.2351	0.2738
0.8674	0.1607	0.2022	0.2205	0.2558
0.9641	0.1522	0.1908	0.2074	0.2398
1.005	0.1490	0.1865	0.2024	0.2338
1.173	0.1374	0.1713	0.1853	0.2134
1.275	0.1316	0.1638	0.1770	0.2034
1.333	0.1286	0.1600	0.1727	0.1984
1.408	0.1250	0.1555	0.1677	0.1926
2.506	0.0945	0.1178	0.1273	0.1465

The mean free path (t_{MFP}) is the average distance that moving particles (such as photons) travel before experiencing a significant change in their direction or energy. Therefore, the t_{MFP} is an essential feature in radiation materials because it shows how photons can interact with materials. Low t_{MFP} means good materials for shielding, and vice versa. Fig. 3 depicts the behavior of the t_{MFP} at various photon energies for *X*- and gamma- rays. The t_{MFP} for the *X*-ray characteristic energies showed an increase in their values. For free PbO glass, the t_{MFP} rose from 0.005 to 0.1477 cm when the *X*-ray energy varied from 8.04 to 50.38 KeV. The effect of PbO on the glass construction impacted the t_{MFP} value. For instance, at an *X*-ray energy of 13.37 KeV, the t_{MFP} reduced from 0.0121 to 0.0052 cm, which the PbO introduced and increased from 0 to 15%. It is noted that at 36.39 KeV, there is a maximum t_{MFP} value of 0.1808 cm for the free PbO sample. This is due to the possible K-absorption edge of Ba.

The same behavior was observed for the gamma-ray energies ranging from 59.54 KeV to 2.506 MeV. The t_{MFP} values have higher values than those detected in X-ray energies. At an energy of 59.54 KeV, the t_{MFP} of the free PbO was 0.2258 cm and increased to 10.5732 cm at 2.506 MeV. The introduction of PbO (15PbO sample) to the glass network reduces the t_{MFP} value, which is reduced to 6.8244 cm at 2.506 MeV. From these results, the introduction of PbO to the network can reduce the t_{MFP} by 1.5 times at high gamma-ray energy (2.506 MeV). As a result, the presence of PbO in the zinc phosphate network lowers the t_{MFP} values, making it more suitable for use as a reducing t_{MFP} through glasses.

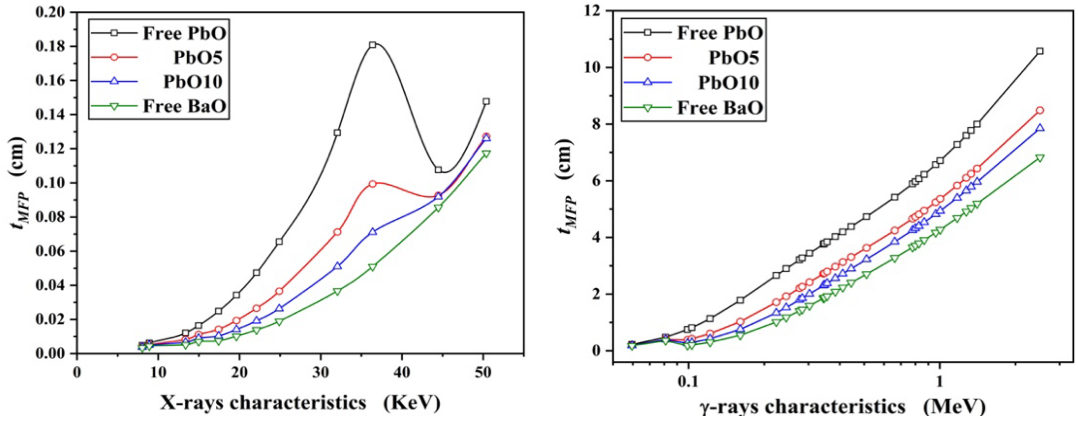

Fig. 3. The mean free path behavior of different barium and lead containing zinc phosphate glass compositions.

The half (t_{HVL}) and tenth (t_{TVL}) value layers are important parameters that show how the glass thickness can reduce the intensity of the radiation to its 1/2 and 1/10 value. As a result, the t_{HVL} and t_{TVL} are critical radiation parameters. As shown in equations 11 and 12, the t_{HVL} and t_{TVL} are both derived from the t_{MFP}. As a result, the behavior of t_{HVL} is similar to that of t_{MFP}. Fig. 4 depicts the relationship between the t_{HVL} and photon energy. When the BaO in zinc phosphate glass was replaced with PbO at 8.04 KeV, the t_{HVL} decreased from 0.0033 cm to 0.0023 cm. When the energy was increased to 81 KeV, the t_{HVL} increased to 0.3308 cm for free PbO glass and 0.252 cm for free BaO glass. Since all glasses exhibit a good reduction of intensity to half value at low photon energies.

The t_{HVL} increases with photon energy from 81 KeV to 2.506 MeV, becoming 7.3272 cm for the free PbO sample and 4.73 cm for the free BaO sample. As a result, the glass containing PbO performs better than the free PbO sample in the Compton scattering process because the quenching of the radiation intensity requires a lower thickness of the free BaO sample than the free PbO glass.

The t_{TVL} values, on the other hand, are shown in Table 3 and follow the same trend as the t_{HVL} in reducing radiation intensity to the tenth value. At a low photon energy of 59.54 KeV, the best thickness for reducing intensity by 90% is 5.2 mm for all glass samples. If the glass contains no BaO, the only layer that can reduce the intensity by 90% is 4.1 mm. At 661.7 KeV, the t_{TVL} value of the free PbO sample was 12.48 cm, which was reduced to 1.65 times in the free BaO samples. Furthermore, at 2.506 MeV, the t_{TVL} of the free PbO glass decreased to 24.35 cm and reached 15.72 cm for the free BaO glass.

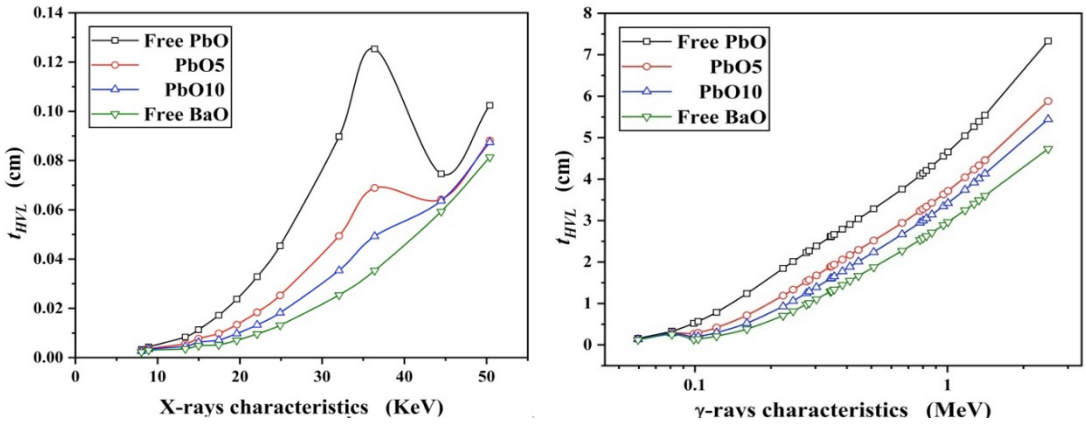

Fig. 4. The half value layer (t_{HVL}) behavior at different energies.

Table 3. The TVL values of $ZnO–P_2O_5$ glass containing BaO and PbO at different photon energies.

Photon energy, ***E*** **(MeV)**	***TVL*** **(cm)**			
	Free PbO	**PbO5**	**PbO10**	**Free BaO**
0.00804	0.0109	0.0090	0.0086	0.0077
0.01337	0.0278	0.0189	0.0153	0.0119
0.0221	0.1089	0.0611	0.0442	0.0319
0.03639	0.4165	0.2289	0.1637	0.1175
0.04448	0.2479	0.2134	0.2116	0.1971
0.05038	0.3403	0.2929	0.2904	0.2704
0.05954	0.5202	0.4464	0.4410	0.4094
0.081	1.0994	0.9336	0.9126	0.8374
0.09897	1.7213	0.8842	0.6124	0.4318
0.103	1.8725	0.9675	0.6724	0.4742
0.2234	6.1228	3.9438	3.0815	2.3403
0.3029	7.9239	5.5709	4.6192	3.6617
0.4111	9.6594	7.2057	6.2566	5.1479
0.511	10.9044	8.3651	7.4333	6.2293
0.6617	12.4818	9.7819	8.8567	7.5484
0.7789	13.5644	10.7293	9.7938	8.4086
0.8674	14.3289	11.3869	10.4398	9.0004
0.9641	15.1267	12.0696	11.1030	9.6025
1.005	15.4562	12.3480	11.3730	9.8465
1.173	16.7554	13.4369	12.4226	10.7919
1.275	17.4953	14.0541	13.0106	11.3179
1.333	17.9037	14.3898	13.3309	11.6027
1.408	18.4134	14.8071	13.7247	11.9518
2.506	24.3500	19.5439	18.0803	15.7166

6. Conclusion

In this study, glasses composed of zinc phosphate, aluminum oxide, lead oxide, and barium oxide were successfully produced. The introduction of PbO to the network caused a significant change in the glass density. The sample of free PbO content had 2.422 g/cm^3, which increased to 3.646 g/cm^3 when PbO replaced BaO content. The variation in the glass density could be related to the enhancement of the bridging oxygen and the replacement of the lower BaO density with the higher PbO density. The Makishima-Mackenzie approximation was used to evaluate elastic parameters. The increase in Young's modulus, bulk modulus, and shear modulus values from 52.82 GPa to 69.648 GPa, 29.48 GPa to 52.7 GPa, and 23.59 GPa to 29 GPa, where the glass composition changed from free PbO to free BaO, indicates that the addition of PbO strengthened the elastic and mechanical properties of such glass. When BaO was replaced by PbO, the Poisson's ratio and hardness value increased slightly from 0.198 to 0.28 and from 3.371 GPa to 4.954 GPa, respectively, confirming the cross-linking glass network.

The addition of BaO and PbO to zinc phosphate glass improved its radiation efficiency. The presence of PbO improves the network's radiation parameters. Along with the glass composition, photoelectric and Compton scattering processes dominate the mass attenuation coefficient behavior. For all glass samples, the optimal thickness for high gamma-ray energy at 661.7 KeV to reduce its intensity by half is approximately 3.75 cm. The half-value layer for free BaO glass, however, measures 4.73 cm at 2.506 MeV. The effective atomic number depends on the ratio of PbO, BaO, or both in the glass network and the scheme of the process. Free BaO glass had the highest effective atomic number of 49.611 at 24.9 KeV. In the field of solid-state radiation, these glasses hold great promise.

Acknowledgements

This research work was funded by Institutional Fund Projects under grant no. IFPIP: 1619-135-1443. The authors gratefully acknowledge technical and financial support provided by the Ministry of Education and King Abdulaziz University, DSR, Jeddah, Saudi Arabia.

References

[1] E. A. Abdel Wahab, A. A. El-Maaref, Kh. S. Shaaban, J. Börcsök, M. Abdelawwad, Optical Mater. **111**, 110638 (2021); https://doi.org/10.1016/j.optmat.2020.110638
[2] X. Li, Z. Xiao, M. Luo, X. Dong, T. Du, Y. Wang, J. Non-Cryst. Solids **469**, 62 (2017); https://doi.org/10.1016/j.jnoncrysol.2017.04.023
[3] S. S. Das, P. K. Srivastava, N. B. Singh, J. Non-Cryst. Solids **358**(21), 2841 (2012); https://doi.org/10.1016/j.jnoncrysol.2012.05.031
[4] N. Azizabadi, P. A. Azar, M. S. Tehrani, P. Derakhshi, J. Non-Cryst. Solids **556**, 120568 (2021); https://doi.org/10.1016/j.jnoncrysol.2020.120568
[5] A. M. El-Khayatt, H. A. Saudi, N. H. AlRowis, Sustainability **15**(12), 9245 (2023); https://doi.org/10.3390/su15129245
[6] K. A. Matori, M. I. Sayyed, H. A. A. Sidek, M. H. M. Zaid, V. P. Singh, J. Non-Cryst. Solids **457**, 97 (2017); https://doi.org/10.1016/j.jnoncrysol.2016.11.029
[7] S. Arivazhagan, K. A. Naseer, K. A. Mahmoud, K. V. A. Kumar, N. K. Libeesh, M. I. Sayyed, M. S. Alqahtani, E. S. Yousef, M. U. Khandaker, Radiat. Phys. Chem. **196**, 110108 (2022); https://doi.org/10.1016/J.RADPHYSCHEM.2022.110108
[8] S. N. Nazrin, A. Sharma, S. Muhammad, N. A. Alghamdi, S. Wageh, Radiat. Phys. Chem. **198**, 110222 (2022); https://doi.org/10.1016/J.RADPHYSCHEM.2022.110222
[9] V. Zanganeh, Optik **269**, 169900 (2022); https://doi.org/10.1016/J.IJLEO.2022.169900
[10] A. Makishima, J. D. Mackenzie, J. Non-Cryst. Solids **17**, 147 (1975); https://doi.org/10.1016/0022-3093(75)90047-2
[11] A. Makishima, J. D. Mackenzie, J. Non-Cryst. Solids **12**, 35 (1973); https://doi.org/10.1016/0022-3093(73)90053-7
[12] S. Inaba, S. Fujino, J. Am. Ceram. Soc. **93**, 217 (2010); https://doi.org/10.1111/j.1551-2916.2009.03363.x
[13] S. Toyoda, S. Fujino, K. Morinaga, J. Non-Cryst. Solids **321**, 169 (2003); https://doi.org/10.1016/S0022-3093(03)00174-1
[14] R. D. Shannon, C. T. Prewitt, Acta Crystallogr. B **26**, 1046 (1970); https://doi.org/10.1107/S0567740870003576
[15] R. D. Shannon, C. T. Prewitt, Acta Crystallogr. B **25**, 925 (1969); https://doi.org/10.1107/S0567740869003220
[16] M. Yamane, J. D. Mackenzie, J. Non-Cryst. Solids **15**, 153 (1974); https://doi.org/10.1016/0022-3093(74)90044-1
[17] M. J. Berger, J. H. Hubbell, XCOM: Photon Cross Sections on a Personal Computer 1987, https://doi.org/10.2172/6016002
[18] M. J. Berger, H. H. Hubbell, S. M. Seltzer, J. Chang, J. S. Coursey, R. Sukumar, D. S. Zucker, K. Olsen, XCOM: Photon Cross Sections Database; https://doi.org/10.18434/T48G6X
[19] M. I. Sayyed, B. Albarzan, A. H. Almuqrin, A. M. El-Khatib, A. Kumar, D. I. Tishkevich, A. V. Trukhanov, M. Elsafi, Materials **14**, 3772 **(**2021); https://doi.org/10.3390/MA14143772
[20] H. O. Tekin, O. Kilicoglu, E. Kavaz, E. E. Altunsoy, M. Almatari, O. Agar, M. I. Sayyed, Results Phys. **12**, 1797 (2019); https://doi.org/10.1016/J.RINP.2019.02.017
[21] J. H. Hubbell, X-Ray Spectrometry **28**, 215 (1999); https://doi.org/10.1002/(SICI)1097-4539(199907/08)28:4<215::AID-XRS336>3.0.CO;2-5
[22] J. H. Hubbell, Phys. Med. Biol. **44**, R1 (1999); https://doi.org/10.1088/0031-9155/44/1/001
[23] A. Un, T. Caner, Ann. Nucl. Energy **65**, 158(2014); https://doi.org/10.1016/J.ANUCENE.2013.10.041

[24] S. Ravangvong, N. Chanthima, Y. Tariwong, J. Kaewkhao, Mater. Today Proc. **4**, 6415 (2017); https://doi.org/10.1016/J.MATPR.2017.06.147
[25] J. S. Hassan, M. Hafid, Mater. Res. Bull. **39**, 1123 (2004); https://doi.org/10.1016/J.MATERRESBULL.2004.02.006
[26] A. Aboalatta, J. Asad, M. Humaid, H. Musleh, S. K. K. Shaat, Kh. Ramadan, M. I. Sayyed, Y. Alajerami, N. Alsahoudi, Nucl. Eng. Technol. **53**, 3058 (2021); https://doi.org/10.1016/J.NET.2021.04.002
[27] M. A. Imheidat, M. KhHamad, K. A. Naseer, M. I. Sayyed, N. Dwaikat, K. Cornish, Y. S. Alajerami, M. Alqahtani, M. H. A. Mhareb, Optik **268**, 169774 (2022); https://doi.org/10.1016/J.IJLEO.2022.169774
[28] H. A. Sidek, R. El-Mallawany, K. A. Matori. M. K. Halimah, Results Phys. **6**, 449 (2016); https://doi.org/10.1016/J.RINP.2016.07.014
[29] A. M. A. Mostafa, S. A. M. Issa, M. I. Sayyed, J. Alloys Compd. **708**, 294 (2017); https://doi.org/10.1016/J.JALLCOM.2017.02.303
[30] J. Singh, V. Kumar, Y. K. Vermani, M. S. Al-Buriahi, J. S. Alzahrani, T. Singh, Ceram. Int. 47, 21730 (2021); https://doi.org/10.1016/J.CERAMINT.2021.04.188
[31] A. B. Chilton, J. K. Shultis, R. E. Faw. "Principles of Radiation Shielding", Prentice Hall, New Jercy, 1984.
[32] M. I. Sayyed, S. Hashim, K. G. Mahmoud, A. Kumar, Optik **274**, 170532 (2023); https://doi.org/10.1016/J.IJLEO.2023.170532
[33] S. A. Bassam, K. A. Naseer, V. K. Keerthana, T. P. Evangelin, C. S. S. Sangeeth, K. A. Mahmoud, M. I. Sayyed, M. S. Alqahtani, E. El Shiekh, M. U. Khandaker, Radiat. Phys. Chem. 206, 110798 (2023); https://doi.org/10.1016/J.RADPHYSCHEM.2023.110798